

PRESENTACION ORAL

Multi-modal DEM in the solar corona

F.A. Nuevo^{1,2}, A.M. Vásquez^{1,2}, R.A. Frazin³, E. Landi³

(1) Instituto de Astronomía y Física del Espacio (IAFE),
CONICET-UBA, Buenos Aires, Argentina

(2) Facultad de Ciencias Exactas y Naturales (FCEN), UBA, Buenos
Aires, Argentina

(3) Department of Atmospheric, Oceanic and Space Sciences, University
of Michigan, Ann Arbor, MI 48109, USA.

Abstract. *Differential emission measure tomography* (DEMT) uses time series of coronal EUV images covering a full solar rotation to determine the three-dimensional (3D) distribution of the *local differential emission measure* (LDEM). The LDEM of each tomographic voxel is a measure of the thermal distribution of the plasma within the cell. The LDEM inversion problem is under-determined and solved by modeling the LDEM as a function with free parameters. In this work we implemented unimodal and non-unimodal LDEM models constrained by data of 3 to 4 bands of the *Atmospheric Imaging Assembly* (AIA) instrument on board the *Solar Dynamics Observatory* (SDO) mission. Our study reveals a multi-modal nature of the LDEM distribution of the global coronal plasma at the tomographic resolution level.

Resumen. La *tomografía de la medida de emisión diferencial* (DEMT) utiliza series temporales de imágenes coronales EUV durante una rotación solar completa para determinar la distribución tri-dimensional (3D) de la *medida de emisión diferencial local* (LDEM). La LDEM de cada celda constituye una medida de la distribución térmica del plasma existente en la misma. El problema de inversión de la LDEM a partir de un bajo número de bandas EUV es sub-determinado, por lo que la LDEM se modela como una función con parámetros libres. En este trabajo implementamos parametrizaciones unimodales y no-unimodales de la LDEM condicionadas por datos de hasta 4 bandas del instrumento *Atmospheric Imaging Assembly* (AIA) a bordo de la misión *Solar Dynamics Observatory* (SDO). Nuestro estudio revela la naturaleza multimodal de la distribución LDEM del plasma coronal al nivel de la resolución tomográfica.

1. DEMT and the LDEM Models

Here we provide a brief introduction to the DEMT technique, for a detailed explanation see Frazin et al. (2009). The inner corona (1.0 - $1.25 R_{\odot}$) is discretized on a spherical grid with a voxel size of 2° in the angular directions and $0.01 R_{\odot}$ in the radial one. A time series of EUV images (Figure 1) covering a

full solar rotation is tomographically inverted to find the value of the *filter band-emissivity* (FBE) $\zeta_i^{(k)}$, at each tomographic voxel i and for each band k . Any given voxel of the tomographic grid is threaded by many coronal magnetic loops, and the plasma contained in it will not be isothermal. The LDEM $\xi_i(T)$ is a measure of the temperature distribution within the voxel i . As shown in Frazin et al. (2009) the FBE and the LDEM are related by

$$\zeta_i^{(k)} = \int dT Q_k(T) \xi_i(T), \quad (1)$$

where $Q_k(T)$ is the *temperature response function* (TRF) of the band (Fig. 1).

Due to the limited number of available bands the inversion of LDEM function is of an under-determined nature. The solution is implemented by modeling the LDEM by a family of functions $\xi_i(T) = F(T, \lambda_i)$, depending on a vector of parameters λ_i . In each tomographic voxel i the problem consists in finding the values of the parameters λ_i that allow to better reproduce the tomographically reconstructed values of FBE in that voxel for all bands. An objective function is defined, that measures the quadratic differences between the tomographic emissivities and the emissivities synthesized from the modeled LDEM.

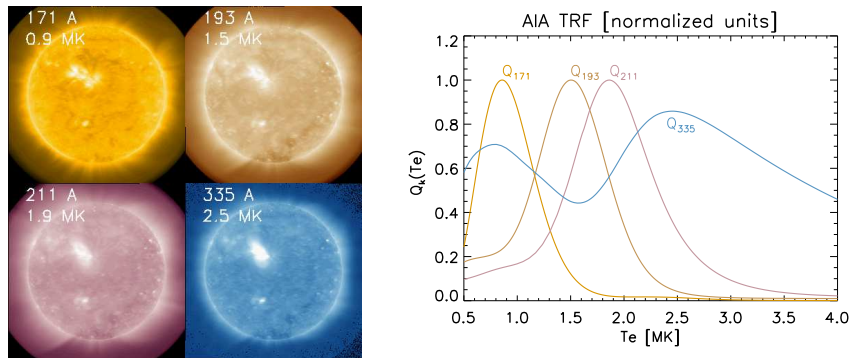


Figure 1. *Left:* An example of EUV images for the 4 AIA bands used in this work. *Right:* TRF of the AIA bands.

We implemented different parametric models $F(T, \lambda)$:

- Single normal function (named “1-normal” hereafter):

$$\xi(T) = A \mathcal{N}(T; [T_0, \sigma_T]), \quad (2)$$

where $\mathcal{N}(T)$ is the normal distribution of centroid T_0 and standard deviation σ_T , and A is a free multiplicative amplitude. This model will be applied when using the 3 bands: 171, 193 and 211 Å, a selection of bands named “AIA-3” hereafter. This is the same parametric model used for all previous DEMT work based on data provided by the (similar) 3 bands of the *Extreme Ultraviolet Imager* (EUVI) on board the *Solar TERrestrial RElations Observatory* (STEREO) mission (Vásquez et al. 2011).

- Double normal function (named “2-normal” hereafter):

$$\xi(T) = A_1 \mathcal{N}_1(T; [T_{0,1}, \sigma_{T1}]) + A_2 \mathcal{N}_2(T; [T_{0,2}, \sigma_{T2}]), \quad (3)$$

being a superposition of two normal functions. The first one has 3 free parameters (as in the previous item). The second one has 2 free parameters (amplitude and centroid), with its standard deviation set at $\sigma_{T2} \approx 0.25$ MK (which is half the temperature step between the peak response of the consecutive AIA bands 211 and 335 Å). This model has then a total of 5 free parameters, and will be applied when using the 4 AIA bands: 171, 193, 211 and 335 Å, a set named “AIA-4” hereafter.

- Other unimodal functions: For AIA-4 we experimented other unimodal functions, specifically: a) “top hat” distribution, characterized by 4 parameters; and b) “top-hat” distribution multiplied by a power law, characterized by 5 parameters to achieve unimodal asymmetrical distributions.

Once the LDEM is determined at every voxel i , we derive the squared electronic density (N_e^2) and the mean electronic temperature (T_m) by taking the first two moments of the distribution over temperature (Frazin et al. 2009). We also compute at every voxel i the following score, as a measure the degree of success of the LDEM in reproducing the tomographically reconstructed FBEs,

$$R_i \equiv (1/K) \sum_{k=1}^K \left| 1 - \zeta_{i,\text{syn}}^{(k)} / \zeta_{i,\text{tom}}^{(k)} \right|, \quad (4)$$

where $\zeta_{i,\text{tom}}^{(k)}$ y $\zeta_{i,\text{syn}}^{(k)}$ are the tomographic and synthetic FBEs. A perfect fit implies $R = 0$, and the higher the score the poorer the fit.

2. Results and Conclusions

We performed DMT analysis of the *Carrington rotation* (CR) 2099 (2010, 13 July through 09 August), during the early rising phase of solar cycle 24 using AIA data. This period is one of the earliest periods for which full data from AIA is available, and the most quiet period observed by that instrument, which is preferred for global DMT analysis.

Figure 2 shows the DMT results at a sample height of $1.115 R_\odot$ using the following sets of filters and LDEM models: AIA-3/1-normal and AIA-4/2-normal. Similar maps are also obtained at all 25 height bins of the tomographic grid. We over-plot the boundaries between magnetically open and closed regions using a potential extrapolation (Toth et al. 2011), indicated as thick black curves. While the morphology of the corona is clearly more complex compared to solar minimum, there is an overall good agreement between the magnetic and the density/temperature-DMT structures. Closed structures are characterized by larger values of both density and temperature.

The differences seen in Figure 2 between the results obtained with AIA-3/1-normal and with AIA-4/2-normal data sets are mainly due to the inclusion of AIA 335 Å band, sensitive to temperatures higher than the other three bands. As can be qualitatively seen in the left and central panels of Figure 2, the AIA-4/2-normal results have systematically larger values of N_e and T_m respect to the

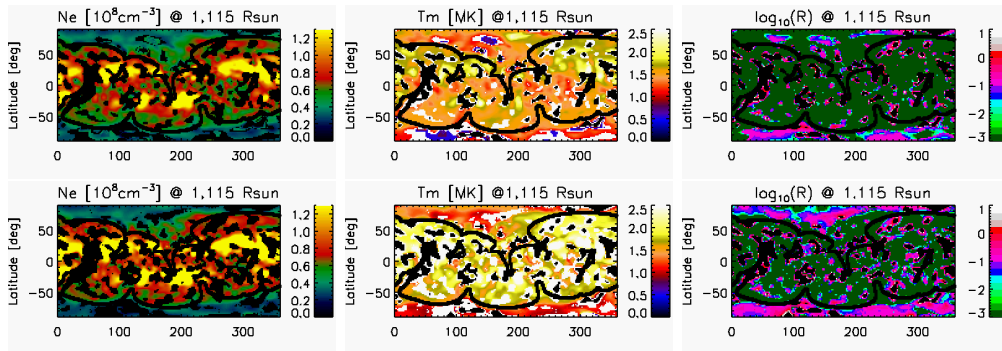


Figure 2. Period CR-2099. Carrington maps of N_e , T_m and the score R at $1.115 R_\odot$ using data of AIA-3/1-normal (top) and AIA-4/2-normal (bottom).

results obtained with AIA-3/1-normal. The systematic increment in the LDEM moments is more significant in the closed region, where the hotter plasma is located and, as a consequence, the second normal function contains more plasma.

Using the AIA-3 set and the 1-normal parametrization, the level of success is very similar to previous DEMT studies based on EUVI data, with a median value of $R_{\text{MED}} = 1.1 \times 10^{-3}$, and with 99% of the coronal volume having very low scores $R < 5 \times 10^{-3}$ (dark-green area in the top-right panel of Figure 2).

Using the AIA-4 set we tested several unimodal models, both symmetrical (1-normal, top-hat) and asymmetrical (top-hat times a power law). We do not include the maps here due to lack of space, but in all cases we obtain $R_{\text{MED}} \gtrsim \times 10^{-1}$ and more than 75% of the voxels having $R > 5 \times 10^{-2}$. In other words, unimodal models are a much poorer description of the information provided by the AIA-4 set over the temperature sensitivity range they provide, which is expanded respect to the AIA-3 set. When using the 2-normal distribution, the very high level of success is recovered: $R_{\text{MED}} = 1.1 \times 10^{-3}$ and 91% of the voxels having $R < 5 \times 10^{-3}$ (dark-green area in the bottom-right panel of Figure 2). Summarizing, at the tomographic resolution the corona emissivity seen in all 4 AIA bands can only be explained with bi-modal LDEM distributions.

The modest temporal resolution of the tomographic technique does not allow to discriminate if the successful bi-modal distribution is the result of unresolved dynamics along magnetic loops, or if it represents plasma simultaneously located along different loops. To investigate these issues, we are currently performing DEM analysis of AIA image sets using the same approach of this work (Nuevo et al. 2014). Future planned work is the combination of the DEMT results with magnetic models under the stationary assumption. Such an approach will allow derivation of the 3D distribution of the heating rate of the quiet corona.

References

- Frazin R. A., et al., 2009, ApJ, 701, 547
 Nuevo F. A, et al., 2014, ApJ, in preparation
 Toth G. et al., 2011, ApJ, 755, 86
 Vázquez A. M, et al., 2011, Solar phys., 274, 259